Numerical Inversion of the Spherical Radon Transform

UNIVERSITÄT DES SAARLANDES

A. K. Louis, M. Riplinger

Institute for Applied Mathematics, Saarland University, 66123 Saarbrücken, Germany

E-mail: louis@num.uni-sb.de / riplinger@num.uni-sb.de

IAM Institut für Angewandte Mathematik

joint DFG project with E. Spodarev, M. Spiess (Institute of Stochastics, Ulm University)

Spherical Radon transform

It is defined by

$$R : L_e^2(\mathcal{S}^2) \longrightarrow L_e^2(\mathcal{S}^2),$$
$$Rf(\eta) = \frac{1}{2\pi} \int_{\langle\omega,\eta\rangle=0} f(\omega)\, w_2^{\eta^\perp}(d\omega).$$

$w_2^{\eta^\perp}(\cdot)$ surface area measure on the subsphere $\mathcal{S}^2 \cap \eta^\perp$,

$L_e^2(\mathcal{S}^2)$ even functions in L^2 over the sphere $\mathcal{S}^2$.

Properties of the transform

The spherical Radon transform

- is a linear, continuous operator,
- is self-adjoint, i.e. $R = R^*$,
- is a bijection from $C_e^\infty(\mathcal{S}^2)$ to $C_e^\infty(\mathcal{S}^2)$,
- commutes with rotations, i.e. for all $\phi \in SO_3$ we have

$$R(T_\phi f) = T_\phi Rf$$

with $T_\phi f(x) := f(\phi^{-1}x)$.

Analytic inversion formula

For $g \in C_e^\infty(\mathcal{S}^2)$ the following inversion formula holds

$$g(\xi) = \frac{1}{2\pi}\left(\frac{\partial}{\partial(\mu^2)}\right)\left[\int_{\{\langle\xi,\omega\rangle^2>\mu^2\}\cap\mathcal{S}^2} \frac{Rg(\omega)|\langle\xi,\omega\rangle|}{\{\langle\xi,\omega\rangle^2-\mu^2\}^{1/2}}\,d\omega\right]_{\mu=0}.$$

Problem: This formula cannot be used numerically.

Approximate Inverse

- We are looking for the solution of $Rf = g$.
- Instead of f, we reconstruct an approximate version f_γ with the property

$$f_\gamma \to f \quad \text{as} \quad \gamma \searrow 0.$$

- Solve the auxiliary problem

$$R^*\psi_\gamma(x,\cdot) = R\psi_\gamma(x,\cdot) \stackrel{!}{=} e_\gamma(x,\cdot),$$

with chosen *mollifier* e_γ and *reconstruction kernel* ψ_γ. Then define

$$f_\gamma(x) := \langle f, e_\gamma(x,\cdot)\rangle = \langle g, \psi_\gamma(x,\cdot)\rangle.$$

- Advantages
  - Built in regularization.
  - Auxiliary problem is solvable independent of the rhs g.

This leads to an efficient and stable algorithm.

Desired mollifiers

- The spherical Radon transform is only defined for even functions, so only even mollifiers are applicable.
- Due to the rotational invariance, it suffices to declare e_γ for an arbitrary reconstruction point x. We choose the third unit vector e_3 and consider mollifiers which only depend on the polar angle θ.

Two interesting examples of mollifiers can be seen in the following figures as functions of the polar angle θ.

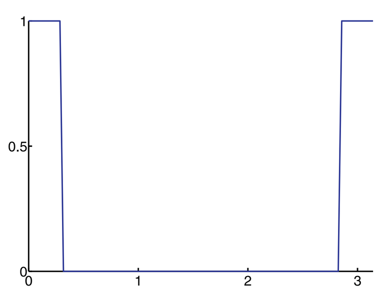

Figure 1: Characteristic mollifier.

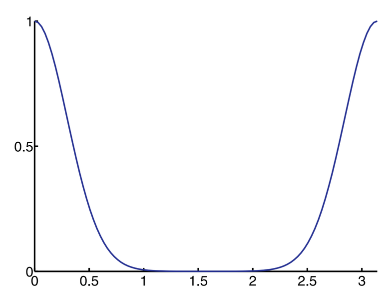

Figure 2: Gauss mollifier.

Reconstruction kernels

- Example 1:

$$\psi_\gamma(e_3, y) = c(\gamma)\cdot\begin{cases} 1, & \text{if } |y_3| < \sin(\gamma), \\ \frac{2\gamma}{2\gamma-\pi}, & \text{else.}\end{cases}$$

The associated mollifier can now be calculated via $R\psi_\gamma = e_\gamma$:

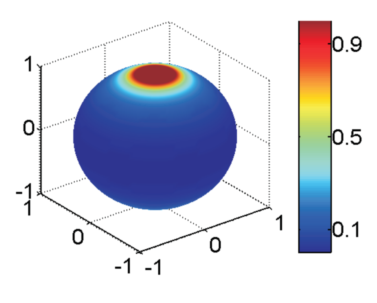

Figure 3: Spherical plot of e_γ.

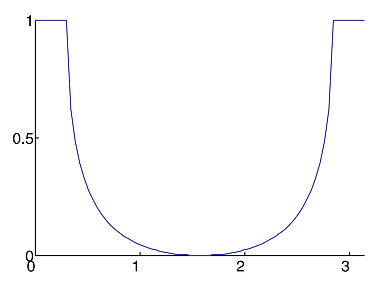

Figure 4: Associated mollifier as function of y_3.

- Example 2:

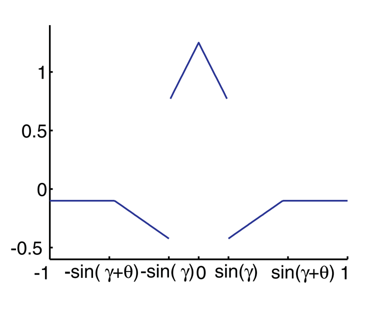

Figure 5: Second reconstruction kernel as function of y_3.

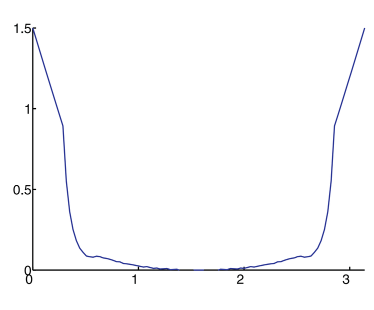

Figure 6: Associated mollifier e_γ as function of y_3.

Numerical integration over the sphere

We use the formula

$$\int_{\mathcal{S}^2} f(\omega)\,d\omega \approx 2\sum_{k=1}^{m}\sum_{l=1}^{n} g(\theta_k,\phi_l)\frac{M(A_k)}{m},$$

with $g(\theta,\phi) := f(\sin(\theta)\cos(\phi), \sin(\theta)\sin(\phi), \cos(\theta))$ for an even function f.

We discretize the sphere as seen in the figure on the right hand side and weight the data with the corresponding surface area.

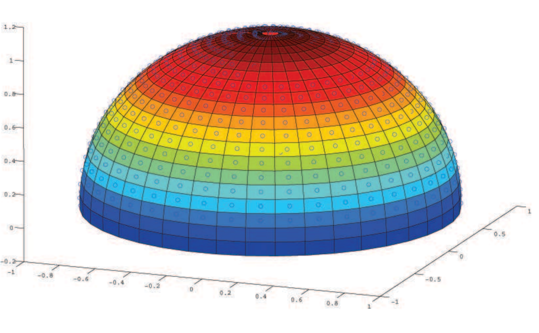

Numerical results

Simulated data

We consider the function

$$f(x,y,z) = \cos(12y)\cdot(1-|z|)$$

to test our algorithm.

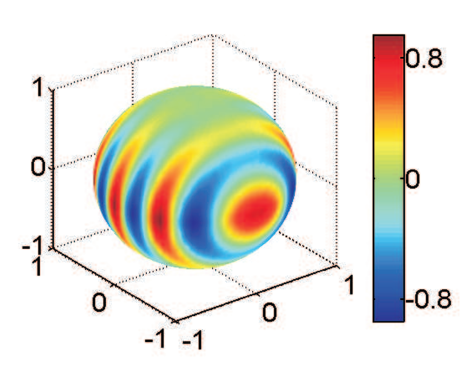

Figure 7: Spherical plot of the data.

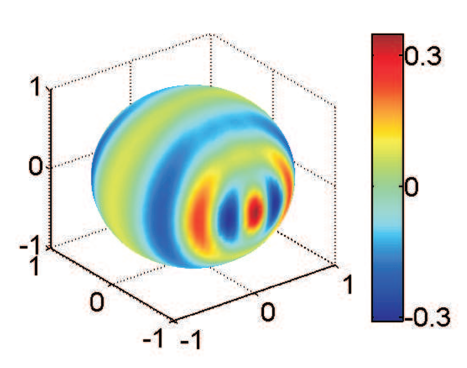

Figure 8: Radon transform of f.

Reconstruction from exact data

We assume knowledge of the exact data at spherical coordinates with polar angle θ_i and azimuth angle ϕ_j:

$$\theta_i = \tfrac{(i-1)\pi}{100}, \qquad i = 1,\dots,50,$$
$$\phi_j = \tfrac{(j-1)2\pi}{100}, \qquad j = 1,\dots,100.$$

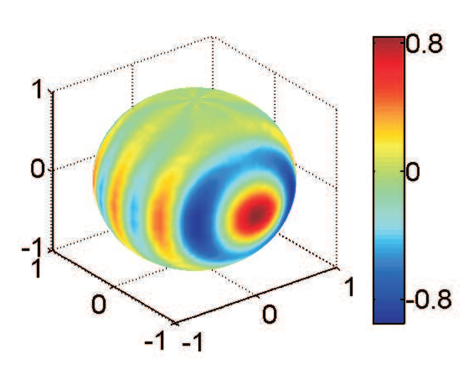

Figure 9: Reconstruction with the first reconstruction kernel ($\gamma = 0.1$).

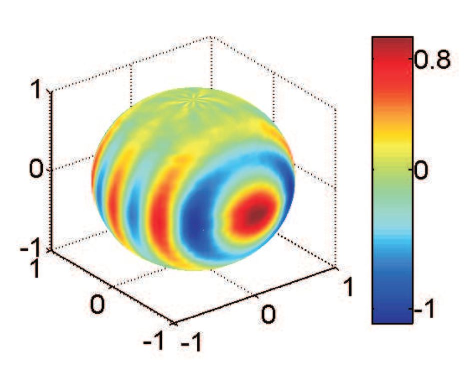

Figure 10: Reconstruction with the second reconstruction kernel ($\gamma = 0.15$).

Reconstruction from noisy data

We perturb the Radon transform of f with various noise and use the second kernel for the reconstruction.

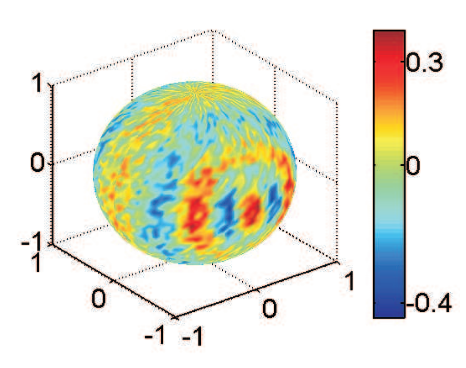

Figure 11: Uniformly distributed noise in [-0.15,0.15].

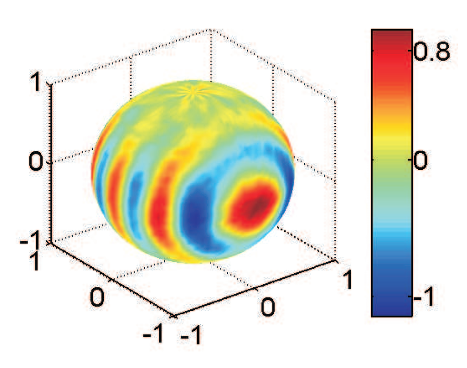

Figure 12: Reconstruction from noisy data.

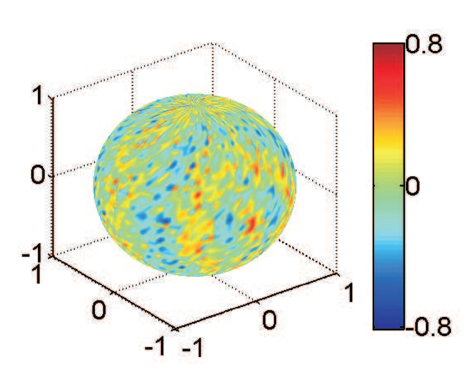

Figure 13: Normally distributed noise with $\sigma = 0.2$.

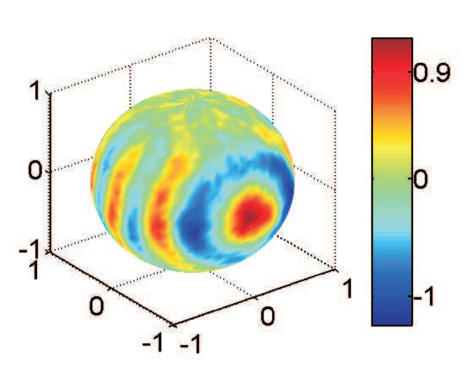

Figure 14: Reconstruction from noisy data .

References

[1] A.K. Louis, "Approximate inverse for linear and some nonlinear problems", *Inverse Problems*, vol. 12, pp. 175-190, 1996.

[2] A.K. Louis, "Combining Image Reconstruction and Image Analysis with an Application to 2D - Tomography", *SIAM J. Imaging Sciences*, vol. 1, pp. 188-208, 2008.

[3] E. Spodarev, "On the rose of intersections of stationary flat processes", *Advances in Applied Probability*, vol. 33, pp. 584-599, 2001.

Deutsche Forschungsgemeinschaft DFG